Fault detection for a switched battery system via constrained nonlinear state estimation

Jonathan Mitchell
School of Aerospace, Mechanical
and Mechatronic Engineering
University of Sydney
Australia
Email: j.mitchell@acfr.usyd.edu.au

Ian Manchester
School of Aerospace, Mechanical
and Mechatronic Engineering
University of Sydney
Australia
Email: i.manchester@acfr.usyd.edu.au

***Abstract*—Accurate Health Usage and Monitoring System (HUMS) for military vehicle batteries is an important enabler for ensuring mission effectiveness and optimising vehicle Through Life Support (TLS). This paper reviews a switched battery system that is typical of some military vehicles and develops two approaches for constructing a diagnostic observer to evaluate battery health; a constrained Extended Kalman Filter (EKF) approach and a Moving Horizon Estimator (MHE) approach. These two approaches are implemented and evaluated against data from a test bench emulating a military vehicle battery system. Both approaches were successful in detecting faults in the dataset, with the performance of both the MHE and EKF near identical. The MHE was capable of having a tighter tolerance on the residual and therefore is more sensitive to faults; However, this was not evident in our results due to the severity of our degraded batteries not exploiting this difference in sensitivity. The MHE approach provides a more natural way to describe the Fault Detection and Isolation (FDI) system, but the EKF performs sufficiently and is both computationally simpler to implement and execute. It was also noted that faulty batteries could only be detected so long as there was an adequate stimulus applied to the system. As such the development of a probing signal to stimulate the system in periods of low stimulus would provide regular assessments of battery health.**

I. Introduction

Fault Detection and Isolation (FDI) in battery systems is an important capability for modern vehicles. This need is prevalent in vehicles with electric and hybrid electric drives [1]. Health estimation in battery systems is also of importance for the power industry for the storage of energy from renewable sources. Such systems contribute to ensuring a reliable power supply uninterrupted by faults. The storage and retrieval of energy in secondary batteries has become ubiquitous as electronics and their energy demands have become integrated into all aspects of society. This growth of embedded electronics has also been seen in military vehicles over the years. These growing electrical demands have largely been due to the modernisation of equipped Command Control Communications Computers Intelligence Surveillance and Reconnaissance (C4ISR) systems supporting Network-Centric Warfare (NCW) [2]. As such, military vehicles exhibit a need, just as electric vehicles do, for robust battery systems to support these energy demands.

A failure in a battery for a military vehicle can lead to its inability to complete its mission, and potentially strand its occupants. Due to the varying nature of vehicle use and mission profile, engine hours is typically not a reliable indicator of battery health. Accurate health and monitoring of military vehicle batteries is thus an important enabler for ensuring mission effectiveness and optimising vehicle Through Life Support (TLS).

This paper explores the application of Fault Detection to a lead-acid switched battery system similar to those used on some military vehicles. The approach taken in this paper was to build a diagnostic observer based FDI system utilising an Equivalent Circuit Model (ECM). Two diagnostic observer approaches were constructed and compared, an Extended Kalman Filter approach and a Moving Horizon Estimation approach. These two observers were then implemented and their performance was evaluated against a dataset generated from a Test Bench representing the vehicle battery system.

This paper is organised into the following Sections: Section I, an introduction. Section II details the switched battery system and the ECM constructed. Section III details the design of the diagnostic observer approaches. Section IV details the implementation of the diagnostic observers. Section V detail the results of the diagnostic observers and their effectiveness. Section VI provides concluding remarks from this paper.

II. Battery Model

With the modernisation of military assets to support Network-Centric Warfare (NCW) [3], military vehicles are being increasingly equipped with modern Command Control Communications Computers Intelligence Surveillance and Reconnaissance (C4ISR) systems. This places strenuous demands on their power systems that weren't originally envisioned during platform acquisition. These C4ISR systems enable military vehicles to reach greater mission effectiveness but also places a risk on their availability due to early degradation and reduced performance of the vehicles battery system. It is thus necessary to provide accurate health monitoring of military vehicle battery systems to mitigate these risks imposed by the power demands of modern C4ISR systems.

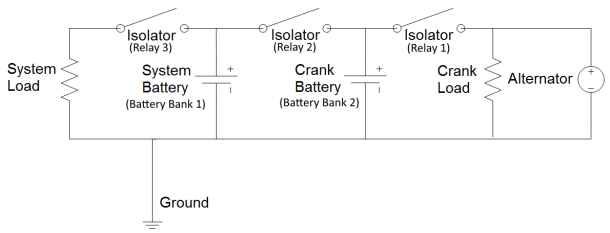

Fig. 1. Military Vehicle Battery System

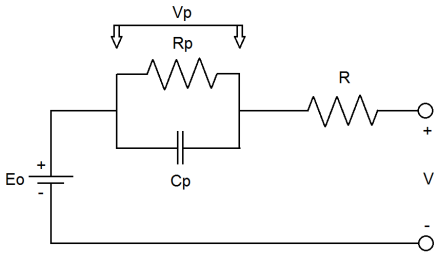

Fig. 2. Battery Equivalent Circuit Model (ECM)

An example of a battery system found on some military vehicles is given in Fig. 1. This is the system configuration assumed for the purposes of developing an Fault Detection and Isolation (FDI) system. This battery system comprises of two lead-acid battery banks, each featuring two batteries in series to provide 24V. A 27V alternator provides power to the main systems when the engine is on and the isolators connected. This system is capable of being isolated into eight configurations due to the presence of the three isolator switches. These isolator switches do not report their position status.

The crank battery is used to power the starter motor for cranking and power vehicle dash electronics. The system battery is used to power the C4ISR systems on the vehicle. The crank battery and system battery can be connected in parallel via an isolator switch which provides additional battery capacity to the C4ISR systems and provides power to the system battery from the alternator.

There are typically two approaches for modelling a battery; an Electrochemical approach that relies on chemical laws and dynamics for describing battery behaviour, or an Equivalent Circuit approach that instead relies on electrical laws and dynamics to describe battery behaviour. The modelling approach chosen for this paper was an ECM. This approach has been used numerously in the literature with successful results [1], [4], [5]. There are many variations on how an ECM for a battery is constructed, including simple voltage source / resistance models, RC network models and Thevinen equivalent models [6].

The ECM chosen for modelling the lead-acid battery was a Thevinen equivalent model (shown in Fig. 2). This ECM comprises of a function $E_o(\text{SoC})$ that models the electromotive force, a resistor R that models the voltage response to current draw, and an RC network (R_p, C_p) that models the time dependant transients and voltage losses due to polarisation [7].

The electromotive force E_o is a piecewise nonlinear function based on State of Charge (SoC) and derived from the formulation given by Plett [8].

$$E_o(\text{SoC}(t)) = \begin{cases} 18.5v & (\text{SoC}(t) \leq 0) \\ 24.8v & (\text{SoC}(t) \geq 1) \\ K_0 - \frac{K1}{\text{SoC}(t)} & \\ +K_2\text{SoC}(t) & \\ +K_3 \ln(\text{SoC}(t)) & (0 < \text{SoC}(t) < 1) \\ +K_4 \ln(1 - \text{SoC}(t)) & \end{cases} \tag{1}$$

Constructing the dynamic equations for the ECM we apply Kirchoff's laws.

$$\begin{aligned} \frac{dV_p}{dt} &= -\frac{1}{R_p C_p} V_p + \frac{1}{C_p} i \\ V &= E_o - Ri - V_p \end{aligned} \tag{2}$$

Where V_p is the voltage across the RC network, R_p and C_p are the resistance and capacitance respectively of the polarisation effects in the battery, R is the internal battery resistance, E_o is the open circuit voltage, V is the terminal voltage and i is the battery current.

To construct the SoC model, we use the current integration method which is a common approach amongst battery modelling literature. The method is straight forward and reliable given accurate current measurements and the availability of re-calibration points [9]. These recalibration points should be used in periods of sustained zero current draw where terminal voltage most accurately represents $E_o(\text{SoC})$. This enhancement was not implemented in this paper but is a recommended addition to a production implementation.

$$S = S_o - \frac{\eta_i}{C_n} \int i(t)\, dt \tag{3}$$

Where $i(t)$ is the current, S_o is the initial SOC, C_n is the nominal battery capacity and η_i is the coulombic efficiency, which is typically $\eta_i = 1$ for discharge and $\eta_i \leq 1$ for charge.

We now have the dynamic Equations (1), (2) and (3) for the ECM which can be approximated in discrete state space form using the Euler Method and a timestep Δt. Process noise w_k and sensor noise v_k have also been added to the model.

$$\begin{aligned} x_{k+1} &= f(x_k, u_k) \\ y_k &= h(x_k, u_k) \end{aligned} \tag{4}$$

$$\begin{aligned} f(x_k, u_k) &= Ax_k + Bu_k + w_k \\ h(x_k, u_k) &= E_o(x_k(2)) - Ru_k - x_k(1) + v_k \end{aligned} \tag{5}$$

$$\begin{aligned} w_k &= \mathcal{N}(0, Q) \\ v_k &= \mathcal{N}(0, R) \end{aligned} \tag{6}$$

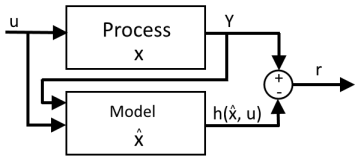

Fig. 3. Model-based fault detection and isolation scheme

$$x_k = \begin{bmatrix} V_p \\ \text{SoC} \end{bmatrix} \qquad u_k = \begin{bmatrix} i \end{bmatrix} \tag{7}$$

$$A = \begin{bmatrix} (1 + \frac{-\Delta t}{R_p C_p}) & 0 \\ 0 & 1 \end{bmatrix} \qquad B = \begin{bmatrix} \frac{-\Delta t}{C_p} \\ \frac{-\eta_i \Delta t}{C_n} \end{bmatrix} \tag{8}$$

The variance for the sensor noise R was estimated from the noise characteristics of the voltage sensor used in the test bench for data collections. The variance of the process disturbances Q was used as a design parameter and tuned for the model to provide a balance between stability and fault sensitivity.

III. Diagnostic Observer

Model based FDI utilises our understanding of physical phenomena and exploits analytical redundancy to generate accurate evaluations of system health. Through describing systems via dynamic models we can monitor this nominal model against the real system performance. Deviations between the nominal model and the actual system can then be used to infer system faults. The general scheme for model-based fault detection and diagnosis is given by Isermann [10]. The scheme used for this paper is shown in Fig. 3.

Diagnostic observers employ an estimator to generate features used for monitoring system faults [11]. Commonly this is a comparison between the estimated output given the dynamic model, versus the actual measured output of the system. The subtracted difference between these two signals is termed the residual. When the residual diverges past a threshold you can infer that a fault in the system has occurred given an adequately robust dynamic model.

Two Diagnostic Observers are compared in this study for an effective FDI system. One method employs a Moving Horizon Estimator (MHE) to generate the residual for the Battery System, whilst the other method employs an Extended Kalman Filter (EKF) to generate the residual. A comparison between the two methods are then presented in Section V.

A. Moving Horizon Estimator

MHE has become a powerful technique for state estimation of dynamic systems in the presence of disturbances, nonlinearities and constraints. A MHE solves the estimation problem by optimising a cost function derived from the dynamic model defined over a sliding window. The sliding window bounds the computation cost of solving the optimisation problem over an infinite time horizon. The cost function is typically comprised of two contributions, an arrival cost that summarises previous data and a prediction error that encapsulates the system dynamics over the defined time horizon. This cost function is then minimised with respect to a set of constraints resulting in a state estimate of the system for the given time horizon [12].

A MHE approach for our Battery System Diagnostic Observer is attractive due to its ability to readily incorporate constraints, such as constraining the SoC between its defined values, and voltage lost (V_p) due to polarisation based on our physical knowledge of batteries. Using our system model definition given by Equations (1), (2) and (3), we can define a MHE as follows for our Battery System.

$$\arg \min_{\hat{x}_{\{k-N:k\}}} \Phi(\bar{x}_{k-N}, y_{\{k-N:k\}}) \tag{9}$$

$$\Phi = ||\hat{x}_{k-N} - \bar{x}_{k-N}||_P^2 + \sum_{i=k-N+1}^{k-1} ||\hat{x}_{i+1} - f(\hat{x}_i, u_i)||_Q^2 + \sum_{i=k-N+1}^{k-1} ||y_i - h(\hat{x}_i, u_i)||_R^2$$

subject to:

$$|V_p| \leq 2.5; \quad 0 \leq \text{SoC} \leq 1; \quad \text{SoC}_{k+1} = \text{SoC}_k + \frac{-\eta_i \Delta t}{C_n}$$

Where $\bar{x}_{k-N}$ is the arrival prediction estimated in the previous timestep $k-1$. P is a weighting matrix penalising the distance in the arrival cost from the previous sliding window estimate. Through out this paper, given a symmetric positive definite matrix M and a vector z; $||z||_M \triangleq (z^T M z)^{(1/2)}$. The constraints placed on SoC is due to its definition, being between 0 and 1, and its update is constrained to the coulomb counting method defined in Equation 3. Errors accumulated over time due to the coulomb counting method can be corrected using regular recalibration points for the SoC. The constraint placed on V_p, the voltage lost due to polarisation effects, has been determined based on nominal polarisation dynamics of the lead-acid batteries used in this Battery System [7].

With the above formulation, we can implement a diagnostic observer based on a MHE approach. Implementation of this diagnostic observer is given in Section IV.

B. Extended Kalman Filter

A common approach to developing a diagnostic observer is to use a Kalman Filter. In this paper we used an EKF to account for nonlinearities in the output equation $h(x_k, u_k)$. With respect to our model, we define our state space system as follows using Equations (1), (2) and (3). Given a model in this form we can implement an EKF [13] as follows.

First we initialise the filter:

$$\begin{aligned} \hat{x}_0^+ &= \mathbb{E}[x_0] \\ P_o^+ &= \mathbb{E}[(x_0 - \hat{x}_0^+)(x_0 - \hat{x}_0^+)^T] \end{aligned} \tag{10}$$

For $k = 1, 2, 3, ...$ we calculate the following.
(a) Compute the time update for both the state estimate and the estimation error covariance as follows:

$$\hat{x}_k^- = A\hat{x}_{k-1}^+ + Bu_{k-1}$$
$$P_k^- = AP_{k-1}^+ A^T + Q_{k-1} \tag{11}$$

(b) Compute the following partial derivative matrices:

$$H_k = \left.\frac{\partial h}{\partial x}\right|_{\hat{x}_k^-}$$
$$M_k = \left.\frac{\partial h}{\partial v}\right|_{\hat{x}_k^-} \tag{12}$$

(c) Compute the measurement update of the state estimate and the estimation error covariance as follows:

$$L_k = P_k^- H_k^T (H_k P_k^- H_k^T + M_k R_k M_k^T)^- 1$$
$$\hat{x}_k^+ = \hat{x}_k^- + L_k[y_k - h(\hat{x}_k^-, u_k)]$$
$$P_k^+ = (I - L_k H_k) P_k^- \tag{13}$$

With the above formulation, we can implement a diagnostic observer based on an EKF approach. However, it is beneficial to apply similar constraints described from the MHE approach (9) to the EKF based on our knowledge of the system. Such constraints facilitate the detection of faults by constraining the model output to a nominal case and ensuring the EKF doesn't converge to states inconsistent with our physical understanding of the system.

We know that the SoC changes slowly with time and would like to limit the rate of change of this state variable so that it is appropriately proportional to the current draw on the battery system. To achieve this we set the covariance of the process noise Q near zero such that we place absolute trust in the model time update and disregard the sensor contribution to the SoC. This ensures the SoC updates exactly according to the coulomb counting method (Equation 3). This however will result in the SoC possibly diverging from a correct internal state over time. This is a common limitation with such an approach and is resolved using recalibration points to correct the SoC.

We know based on the definition of SoC and the physical limitations of the polarisation effects [7] we can apply hard state constraints to ensure our model is constrained to a realistic operating region.

(d) Apply hard constraints on state estimates using the projection approach [14]:

$$\tilde{x}^- = \arg\min_{\tilde{x}^-} (\frac{1}{2}\tilde{x}^{-T} H \tilde{x}^- - \hat{x}^{+T} H \tilde{x}^-) \tag{14}$$

such that

$$C_{lb} = \begin{Bmatrix} -2.5 \\ 0 \end{Bmatrix} \leq \tilde{x} = \begin{bmatrix} V_c \\ \text{SOC} \end{bmatrix} \leq C_{ub} = \begin{Bmatrix} 2.5 \\ 1 \end{Bmatrix} \tag{15}$$

$$H = \begin{bmatrix} 1 & 0 \\ 0 & 1 \end{bmatrix} \tag{16}$$

Setting the weighting matrix $H = I$ is equivalent to projecting the unconstrained state to the limits C_{lb} and C_{ub}. This allows for a practical implementation to instead saturate the states at the limits C_{lb} and C_{ub}, avoiding the need to solve an optimisation problem. This reduces the computational complexity significantly. An implementation of an EKF based diagnostic observer using these equations is given in Section IV.

TABLE I
DATASET RELAY PROGRESSION

Relay 1	Relay 2	Relay 3	Time (s)
OFF	OFF	OFF	0
ON	OFF	OFF	120
OFF	ON	OFF	240
OFF	OFF	ON	360
OFF	ON	ON	480
ON	ON	OFF	600
ON	OFF	ON	720
ON	ON	ON	840
OFF	OFF	OFF	960
OFF	OFF	OFF	1080

TABLE II
TEST BENCH DATASETS

	Battery Bank 1		Battery Bank 2	
Dataset ID	Battery 1	Battery 2	Battery 1	Battery 2
1	Healthy	Healthy	Healthy	Healthy
2	Healthy	Faulty	Healthy	Healthy
3	Healthy	Healthy	Healthy	Faulty
4	Healthy	Healthy	Faulty	Faulty
5	Faulty	Faulty	Healthy	Healthy

IV. IMPLEMENTATION

To implement and evaluate the two respective approaches for FDI on the Battery system a representative test bench was constructed. The test bench design is representative of the military vehicle battery system given in Figure 1. The test bench uses a variable electronic load to represent the system load, and a variable power supply to represent the alternator. Relays have been used to act as the Isolator switches and are controlled electronically.

A relay progression was designed to stimulate the test bench into the eight possible connection configurations and is given in Table I. Healthy and faulty batteries where switched out in between tests to generate five sets of data. The faulty and healthy batteries in each set of data is given in Table II. This data set has been used to compare the performance of our two Diagnostic Observers.

The faulty batteries used in the test data collection were ones which had been demonstrated to be incapable of accepting and storing sufficient charge.

A. Moving Horizon Estimator

Constructing the MHE diagnostic observer using the formulation in (9) we arrive at Algorithm 1.

Algoirthm 1 has been implemented in MATLAB using YALMIP [15] using the `fmincon` nonlinear solver and executed against the data described in Table II with results on the diagnostic observers performance given in Section V.

Algorithm 1 MHE Diagnostic Observer

procedure EVALUATE BATTERY HEALTH
  for k = N+1, N+2, N+3, N+4, ... **do**
    if Uninitialised **then**
      SoC $= E^{-1}(V_k)$
      $V_{p,k} = 0$
    end if
    Solve $\arg\min_{\hat{x}_{k-N:k}} \Phi(\bar{x}_{k-N}, y_{\{k-N:k\}})$
    $r(t) = Y_k - h(\hat{x_k}, u_k)$
    if $|r(t)| \geq \gamma$ **then**
      $B_{fault,k} = 1$
    end if
    if $\sum(B_{fault,k-Z:k})/Z == 1$ **then**
      Report Battery Fault
    end if
  end for
end procedure

Algorithm 2 EKF Diagnostic Observer

procedure EVALUATE BATTERY HEALTH
  if k = 0 **then**
    $\hat{x}_0^+ = \mathbb{E}(x_0)$
    $\Sigma_{\tilde{x},0}^+ = \mathbb{E}[(x_0 - \hat{x}_o^+)(x_0 - \hat{x}_o^+)^T]$
  end if
  for k = 1,2,3,... **do**
    $[\tilde{x}_k^-, P_k^+] = \text{EKF}(\hat{x}_{k-1}^+, u_{k-1})$
    if $\tilde{x}_k^- > C_{ub}$ **then**
      $\tilde{x}_k^+ = C_{ub}$
    else if $\tilde{x}_k^- < C_{lb}$ **then**
      $\tilde{x}_k^+ = C_{lb}$
    else
      $\tilde{x}_k^+ = \tilde{x}_k^-$
    end if
    $r_k = y_k - h(\tilde{x}_k^+, u_k)$
    if $|r(t)| \geq \gamma$ **then**
      $B_{fault,k} = 1$
    end if
    if $\sum(B_{fault,k-Z:k})/Z == 1$ **then**
      Report Battery Fault
    end if
  end for
end procedure

B. Extended Kalman Filter

We have constructed the EKF using the formulation in Section III-B in Algorithm 2.

This algorithm was implemented in Matlab and run against the data described in Table II with results on the diagnostic observers performance given in Section V.

V. RESULTS

Running the diagnostic observers detailed in Section III over the dataset defined in Table II we obtained the results listed in Table III for fault detection.

TABLE III
DIAGNOSTIC OBSERVER RESULTS

	MHE		EKF	
Dataset ID	Detection Rate	Missed Detection Rate	Detection Rate	Missed Detection Rate
1	N/A	N/A	N/A	N/A
2	65.94%	34.06%	65.75%	34.25%
3	33.13%	66.87%	33.13%	66.87%
4	99.60%	0.40%	99.59%	0.41%
5	99.60%	0.40%	99.60%	0.40%

For the control test data (Dataset ID 1) both Diagnostic Observers successfully estimated the system state and recorded no Faults. As we then progressed through increasingly faulty configurations of the switched battery system our detection rate improved. The model inferred battery faults through the battery's inability to both accept and deliver charge due to its degraded state. This led to a lesser current being drawn by the faulty battery which resulted in a drop in our nominal voltage, causing a discrepancy between model and actual. This discrepancy leads to a non zero residual.

We were able to successfully detect battery faults given adequate stimulus to the battery system. We observe that the performance between the MHE diagnostic observer and the EKF diagnostic observers are close to identical for all cases.

It is important to note that without the implementation of hard constraints, the performance of the EKF was unsatisfactory as the model incorrectly converged to unrepresentative internal states. This is due to the battery model being incapable of reconciling the internal state into anything meaningful given sensor data from a faulty battery. This was seen in datasets 4 and 5 where the polarisation voltage V_p became arbitrarily large in an attempt to reconcile the faulty battery data. Without the application of a hard constraint on the EKF, the residual will not deviate due to a faulty battery.

Alternatively, a tolerance could instead be applied to the internal state V_p in line with the physical bounds for the polarisation voltage but the implementation of a hard constraint is trivial as shown in Section IV-B. This allows us to be consistent with the approach for FDI as shown in Figure 3.

We also compared the EKF and MHE diagnostic observers for sensitivity to faults by comparing the residuals and how tight the tolerance γ can be set. The log values of the residuals for both diagnostics observers were plotted in Figure 4. We can see from this comparison that the MHE diagnostic observer can have an overall tighter tolerance γ. The MHE tolerance can be set to $\gamma = e^{-5.1} = 0.0061$ versus a tolerance for the EKF of $\gamma = e^{-4.2} = 0.0149$. Thus the MHE diagnostic observer is more sensitive to faults, given an accurate estimate of SoC is achieved. This didn't show in our results due to the faulty batteries used in the test bench being so severe that they weren't on the threshold to see a difference between the MHE and EKF diagnostic observers.

A general observation we can make is that the diagnostic observers perform worse when attempting to detect a single

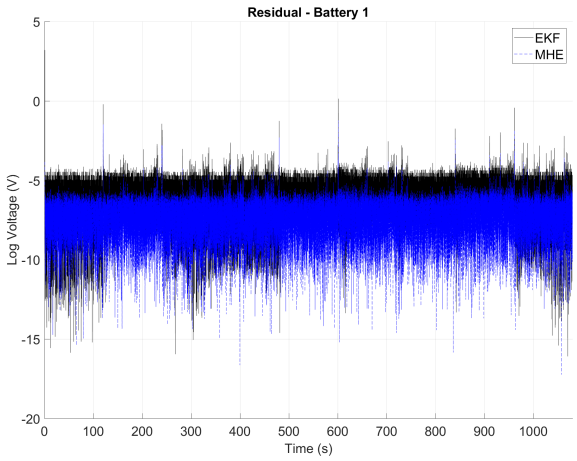

Fig. 4. Residual analysis between EKF and MHE on Dataset 1

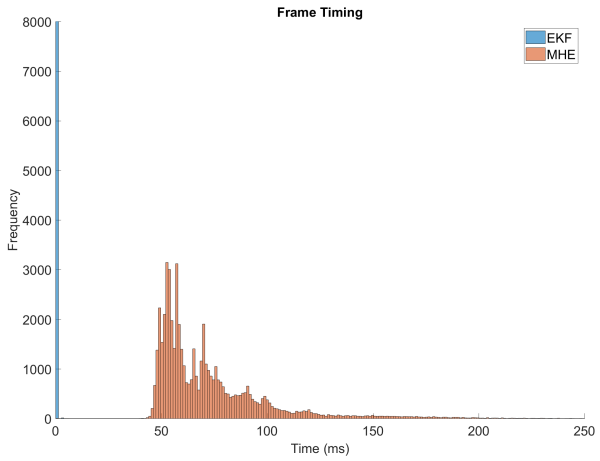

Fig. 5. Histogram of the frame timing for the implemented FDI algorithms

faulty battery in a bank whilst connected in parallel with a healthy battery, but not the alternator. This is due to the healthy battery not providing an adequate potential difference to expose the faulty battery's inability to accept charge, along with the Healthy battery masking the faulty battery by providing the required charge given a connected load. This is observed through the lower detection rates in Dataset IDs 2 and 3. The temporal performance of the diagnostic observers is given in Figure 5. Here we can observe that the EKF outperforms the MHE by two orders of magnitude, which is to be expected given the differences in computational complexity. Given that the ability to detect a battery fault is dependant on having adequate stimulus to excite the system to compare against the nominal model, it would be advisable to regularly poll the batteries and measure their response for performance during periods of low current draw. This provides a routine estimation of battery health and would provide superiour fault detection in the case of inadequate system stimulus. By polling the batteries during no current draw, this opens the paradigm for designing an optimal probe signal to stimulate the battery adequately to provide maximum information for the evaluation of its health. Such an approach has been used successfully for fault detection in other systems [16].

VI. Conclusion

Diagnostic observers were successfully implemented using both an MHE approach and an EKF approach for the battery system described in Figure 1. We found that the MHE approach is slightly more accurate and allows for a tighter tolerance on residual, but a constrained EKF has near identical performance in our test cases and provides a much simpler approach both computationally and in implementation for FDI in this battery system.

Acknowledgment

The authors of this paper would like to acknowledge Thales Australia for supporting this study into Fault Diagnosis in a switched battery system.

References

[1] J. Zhang and J. Lee, "A review on prognostics and health monitoring of Li-ion battery," *Journal of Power Sources*, vol. 196, no. 15, pp. 6007–6014, 2011.

[2] "Future Land Warfare Report," Modernisation and Strategic Planning Division, Commonwealth of Australia, Tech. Rep., 2014.

[3] J. Luddy, "The challenge and promise of Network Centric Warefare," Lexington Institute, Tech. Rep. February, 2005.

[4] M. A. Casacca and Z. M. Salameh, "Determination of lead-acid battery capacity via mathematical modeling techniques," *IEEE Transactions on Energy Conversion*, vol. 7, no. 3, pp. 442–446, 1992.

[5] H. Ham, K. Han, and H. Lee, "Battery System Modeling for a Military Electric Propulsion Vehicle with a Fault Simulation," *Energies*, vol. 6, no. 10, pp. 5168–5181, 2013.

[6] H. He, R. Xiong, and J. Fan, "Evaluation of Lithium-Ion Battery Equivalent Circuit Models for State of Charge Estimation by an Experimental Approach," *Energies*, vol. 4, no. 4, pp. 582–598, 2011.

[7] T. Reddy and D. Linden, *Linden's Handbook of Batteries*, 3rd ed. McGraw-Hill Education, 2010.

[8] G. L. Plett, "Extended Kalman filtering for battery management systems of LiPB-based HEV battery packs: Part 2. Modeling and identification," *Journal of Power Sources*, vol. 134, no. 2, pp. 262–276, 2004.

[9] S. Piller, M. Perrin, and A. Jossen, "Methods for state-of-charge determination and their applications," *Journal of Power Sources*, vol. 96, no. 1, pp. 113–120, 2001.

[10] R. Isermann, "Model-based fault-detection and diagnosis status and applications," *Annual Reviews in Control*, vol. 29, pp. 71–85, 2005.

[11] ——, "Supervision, fault-detection and fault-diagnosis methods An introduction," *Control Engineering Practice*, vol. 5, no. 5, pp. 639–652, 1997.

[12] A. Alessandri, M. Baglietto, G. Battistelli, and V. Zavala, "Advances in moving horizon estimation for nonlinear systems," *49th IEEE Conference on Decision and Control (CDC)*, pp. 5681–5688, 2010.

[13] D. Simon, *Optimal State Estimation*. Hoboken, NJ, USA: John Wiley & Sons, Inc., may 2006.

[14] ——, "Kalman filtering with state constraints: a survey of linear and nonlinear algorithms," *IET Control Theory & Applications*, vol. 4, no. 8, p. 1303, 2010.

[15] J. Lofberg, "YALMIP : a toolbox for modeling and optimization in MATLAB," *2004 IEEE International Conference on Robotics and Automation (IEEE Cat. No.04CH37508)*, no. May, pp. 284–289, 2014.

[16] S. Cheong and I. R. Manchester, "Input design for discrimination between classes of LTI models," *Automatica*, vol. 53, pp. 103–110, 2015.